JJMIE

Volume 19, Number 4, Dec. 2025
ISSN 1995-6665
Pages 733– 747
https://doi.org/10.59038/jjmie/190404
Editor-in-Chief: Prof. Faris M. AL-Oqla

Jordan Journal of Mechanical and Industrial Engineering

Polynomial Regression Machine Learning for Burst Pressure Prediction and Gouge Assessment in API 5L X65 Pipelines

Yassine El Kiri[1*], Zakaria Mighouar[1], Laidi Zahiri[1], Khalifa Mansouri[1]

[1]*Laboratory of Modelling and Simulation of Intelligent Industrial Systems (M2S2I)ENSET, Hassan II University of Casablanca, Morocco.*

Received 13 April 2025 *Accepted 20 September 2025*

Abstract

This study investigated the impact of longitudinal and circumferential gouge defects on pipeline burst pressure. We combined theoretical and numerical analyses with machine learning. Numerical analyses validated the theory. However, the main contribution lies in developing a polynomial regression-based prediction equation. The inclusion of interactions among defect depth, length, and width proved crucial for this equation. It demonstrated excellent performance, achieving correlation coefficients close to 1 on both training and test sets. Compared to numerical approaches, our predictive method reduced the average relative error from 5% to just 1% for longitudinal defects and 2% for circumferential defects. Defect depth is the predominant factor influencing burst pressure, especially for longitudinal defects, thereby confirming their criticality. The overlap of the curves highlights the necessity of considering the combined effect of defect depth and orientation. This research demonstrates the effectiveness of machine learning for predicting burst pressure. The developed equation, once implemented in a mobile application or software, will allow engineers to obtain instant, reliable estimations directly in the field or from a control room. It also advocates a risk-based maintenance approach, prioritizing deep and longitudinal defects.

Keywords: Pipeline,burst pressure, longitudinal gouge,circumferential gouge,finite element analysis, polynomial regression.

Nomenclature

FEA: Finite element analysis.
ANN: Artificial neural network.
p_b:Burst pressure.
r_i:Internal radius of the pipe.
r_e: External radius of the pipe.
R:Radius of the defect curvature of the gouge.
t:Thickness of the pipe wall.
d:Depth of the defect.
w:Half the maximum circumferential length of the defect.
c:Half of the maximum axial length of the defect.
σ_y: Yield Strength.
σ_{uts}: Ultimate Tensile Strength
σ_θ: Circumferential stress.
σ_a: Axial stress.
q:Gouge defect type (longitudinal or Circumferential).
z:Standardized value.
x:Raw Data Value (Non-Standardized).
μ:Average of all values of the characteristic (column).
σ:Standard Deviation of All Values for the Characteristic (Column).
$\sigma_{\mathrm{y\_train}}$: Standard Deviation of Burst Pressure Training Variables.
$\mathrm{y_{train}}$: Burst Pressure Training Variables.
$\bar{\mathrm{y}}_{\mathrm{train}}$: Mean of Burst Pressure Training Variables.
x_{1z}: Standardized Axial Length (Longitudinal Gouge) or Standardized Circumferential Width (Circumferential Gouge).
x_{2z}: Standardized d/t ratio.
x_{3z}: Standardized defect type (longitudinal or circumferential).
x_{4z}: Standardized w/re ratio.
$\mathrm{y_{pred\_z}}$: Standardized prediction of burst pressure via polynomial equation.
$\mathrm{y_{pred}}$: Standardized predicted burst pressure.
$P_{\text{b-theo-long}}$: Theoretical longitudinal burst pressure.
$P_{\text{b-num-long}}$:Numerical Longitudinal Burst Pressure.
$P_{\text{b-theo-circ}}$: Theoretical circumferential burst pressure.
$P_{\text{b-num-circ}}$: Numerical Circumferential Burst Pressure.
$y_{pred-train}$: Burst Pressure Used in Training Data.
$y_{pred-test}$:Burst Pressure Used in Test Data.

1. Introduction

The integrity of gas pipelines, vital infrastructure for global energy supply, is a major concern. Mechanical damage, such as external interference and particularly dent and/or gouge defects, represents a significant threat to the safety and reliability of these systems [1]. These defects can occur during installation, maintenance excavations, or nearby construction work [2]. Mechanical damage, often resulting from negligence or inaccuracy during maintenance, is a frequent cause. If buried pipelines are not

* Corresponding author e-mail: yassine.elkiri-etu@etu.univh2c.ma.

precisely located, they can be struck by construction machinery, and such incidents often go unnoticed or unreported[3]. These defects can lead to significant stress concentrations and weaken the pipelines' burst pressure capacity, directly jeopardizing their operational safety and lifespan. Therefore, accurately assessing their impact is crucial, especially for high-strength steels like API 5L X65, which are widely used in the industry [4-7]. The potential consequences, such as gas leaks, supply interruptions, economic losses, and environmental pollution, underscore the imperative need for precise fitness-for-service evaluations of these damaged pipelines[5-8].

This work, often relying on numerical methods like Finite Element Analysis (FEA), significantly contributes to a better understanding of how these structures behave under stress, which is fundamental for managing the integrity of both gas and oil pipelines [9].

Traditionally, assessing the burst strength of damaged pipelines has relied on various methods. Analytical and semi-empirical approaches, such as ASME B31G or DNV-RP-F101 codes, are popular due to their simplicity. However, they are often criticized for being overly conservative and lacking precision, which can unfortunately lead to unnecessary repairs or an underestimation of the pipelines' remaining service life [5,10,11,12,13]. In parallel, finite element analysis (FEA) has established itself as a benchmark method. It allows for highly accurate modeling of complex defect behavior and precise burst pressure prediction, accounting for material and geometric non-linearity [5,6,11,12,14,15,16,17]. Nevertheless, FEA simulations remain costly in terms of computation time and resources, which limits their application for rapid assessments or large-scale parametric studies.

Figure 1 illustrates the distribution of leak incidents caused by holes over the last 10 years, from 2013 to 2022. External interference incidents represent a significant portion, necessitating thorough research to help pipeline operators act proactively before leaks occur.

The assessment of burst strength for partial wall defects in pipelines originated from work conducted at Battelle in the 1960s and 1970s, which led to the development of failure criteria for through-wall and partial defects based on flow stress and toughness (NG-18 equations) [19]. Several previously published analyses have concluded that the NG-18 equations are the most effective for evaluating partial wall defects, such as gouges [20-21]. The NG-18 equations for partial wall defects are also recommended in the EPRG guidelines for mechanical damage assessment [22].

Despite the growing enthusiasm for machine learning in pipeline integrity management, our literature review highlighted a significant point: most research utilizing Machine Learning for burst pressure prediction primarily focuses on corrosion defects. In contrast, specific applications addressing gouge defects which are critically important for pipelines are almost non-existent. Nevertheless, related studies have explored the use of Machine Learning to predict the burst pressure of pipelines with unconstrained corrosion defects, for both longitudinal and circumferential orientations (Table 1). This body of work confirms Machine Learning's potential for analyzing partial wall defects. It is precisely this gap concerning gouge defects that motivated our study, driving us to develop an innovative approach to address it.

Numerous studies have focused on pipeline failures caused by various types of defects. Among these, extensive research has explored predicting burst pressure in pipelines with complex defects, such as combined dents and cracks.

Table 1. Previous work on pressurized pipelines affected by corrosion:

References	Type	Orientation	Methods
Michael Lo et al. [23] (2022)	Corrosion	Longitudinal	FEA/ANN
Arumugam et al. [24] (2020)		Circumferential	FEA
Arumugam et al. [25] (2020)		Longitudinal	FEA
Xu et al. [26] (2017)		Longitudinal circumferential in interaction	FEA/ANN
Kumar et al. [27] (2022)		Circumferential	FEA/ANN

A gouge on a pipeline, characterized by material removal and work hardening, typically has a high length-to-width ratio and may be angled. It is modeled as a semi-elliptical shape, defined by its length (2c), depth (d), width (2w), and radius (R). The defect is considered critical when the gouge is aligned with the pipeline. Gouges are severe defects. Although sometimes treated as cracks using fracture mechanics (which can underestimate burst pressure), two main approaches are favored: limit analysis and notch fracture mechanics. The precise delineation of their respective application domains remains a challenge [28].

Machine Learning offers powerful tools to address complex problems in mechanical engineering, enabling the modeling of non-linear phenomena and the optimization of intricate systems with increased efficiency [29-33].

Polynomial regression, a Machine Learning technique, is increasingly used to predict complex phenomena. This method allows for modeling non-linear relationships between variables by constructing predictive equations based on training data. Thanks to its adaptability, it proves relevant in many fields where understanding complex relationships is essential, thus offering a more efficient alternative to traditional modeling approaches [33-34].

Facing these limitations, Machine Learning (ML) has emerged as a very promising solution in engineering, capable of enhancing both predictive accuracy and efficiency[14,29,30,31,32]. It is increasingly integrated into Pipeline Integrity Management (PIM) systems for various tasks, such as defect detection, gouge growth prediction, and structural safety assessment[14,36,37,38,39,40,41]. Several ML algorithms, including artificial neural networks (ANN), deep neural networks (DNN) and Support Vector Regression (SVR), have already been investigated to predict the burst pressure of pipelines with gouge defects, showing significant improvements over traditional models[6,10,33,42,43].

Despite the growing interest in machine learning for pipeline integrity management, our literature review highlighted an important point: most research utilizing ML for burst pressure prediction primarily focuses on corrosion defects. In sharp contrast, specific applications addressing gouge defects which are critically important for pipelines are almost non-existent. This precise gap is what motivated our study, driving us to develop an innovative approach to fill this void.

In this study, we present a novel approach to assess the burst pressure of API 5L X65 pipelines, focusing on gouge defects. To overcome the limitations of costly Finite Element Analysis (FEA) and often opaque machine learning models, we developed a polynomial regression equation. We favored this Machine Learning technique for its ability to effectively capture non-linear relationships and crucial interactions among defect parameters (depth, length, and width), while providing an explicit and easily interpretable formula. By combining the precision of our numerical data with the efficiency and transparency of ML, our objective is clear: predict burst pressure affected by gouge defects by Machine Learning then to precisely evaluate the impact of these defects on pipeline integrity, thereby providing a reliable and transparent predictive tool that will improve maintenance decisions for pipelines affected by longitudinal and circumferential gouges defects.

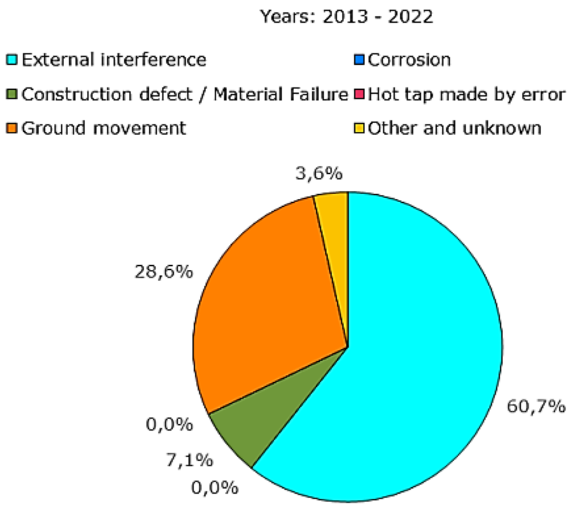

Figure 1. Distribution for incidents with leak size : hole (2013-2022)[18]

2. Materials and methods

Pipelines are susceptible to mechanical damage, including grooves (gouges) as illustrated in Figure 2, resulting from external interference or construction errors [5]. Most damage caused by gouges is geometrically characterized by a 45-degree V-shape rounded at the lower end, idealized as a radius, R, of 2 mm[44].

This defect can occur in different orientations: longitudinal or circumferential. It manifests as a loss of metal and can induce plastic deformation, therefore requiring precise and rigorous evaluation [45].

2.1. Defect assessment

Gouges are mechanical defects caused by contact with a foreign object, resulting in material removal, which can affect the strength of pipelines subjected to internal pressure. Several approaches are available for their assessment (Table 2) [28].

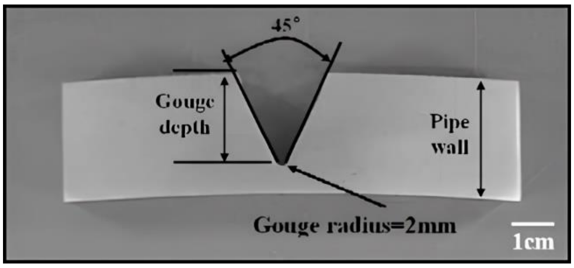

Figure 2. Gouge defect shape in the pipe[5].

Table 2. Recommended Methods for Evaluating the Burst Strength of Gouge Defects in Pressurized Pipelines:

Longitudinal orientation	Circumferential orientation
NG-18 Equation (Kiefner et al., 1973)	Kastner local collapse solution
BS 7910 (BS 7910, 2013)	BS 7910
PAFFC (Leis and Ghadiali, 1994)	API 579
API 579 (API, 2000)	

Burst failure will be evaluated using the NG-18 equation for longitudinal gouge defects and the Kastner equation for circumferential gouge defects. Each equation provides the maximum stress that leads to burst failure of the pipeline. The burst pressure is then deduced from these two stresses using Equations (1) and (2) [46].

$$\sigma_\theta = \frac{p_b . r_i}{t} \quad (1)$$

$$\sigma_a = \frac{p_b . r_i}{2t} \quad (2)$$

2.2. Axial orientation of the gouge defect

In ductile pipelines, the failure stress of an axially oriented V-groove subjected to internal pressure loading is described by Equation 3[47-48] :

$$\sigma_\theta = \bar{\sigma}\frac{1-\frac{d}{t}}{1-\left(\frac{d}{t}\right).M^{-1}} \quad (3)$$

With:

$$M = \sqrt{1 + 0.26.\left(\frac{2.c}{\sqrt{r_e . t}}\right)^2} \qquad \bar{\sigma} = 1{,}15.\sigma_y$$

2.3. Circumferential orientation of the gouge defect

The plastic collapse failure criterion developed by Kastner [49]provides a suitable method for calculating the axial failure stress in the presence of a circumferential groove (positioned 90 degrees from the longitudinal axis) in a ductile pipeline (Equation 4).

$$\sigma_a = \bar{\sigma}\frac{\eta.(\pi - \beta.(1-\eta))}{\pi.\eta + 2.(1-\eta).\sin\beta} \quad (4)$$

With:

$$\bar{\sigma} = 1{,}15.\sigma_y \qquad \beta = \frac{w}{r_e} \qquad \eta = 1 - \frac{d}{t}$$

2.4. Evaluation of Gouge Defects Using the Finite Element Method

The Finite Element Method (FEM) is favored for its accuracy and ability to model complex geometries, heterogeneous materials, and varied conditions, while providing detailed results on the local behavior of structures. Unlike empirical methods, which are limited to specific and approximate cases, FEM is more adaptable and rigorous, particularly useful for advanced 3D analyses.

The analysis was performed using a numerical model implemented in SolidWorks software. A 3D finite element analysis was conducted to simulate the behavior of the pipeline subjected to internal pressure. Calculations focused on evaluating the circumferential and longitudinal stresses in the defective area. Different defect configurations were analyzed by varying their depths and lengths to establish a thorough and accurate analysis between these parameters and burst pressure.

The results of this study will refine the assessment criteria for pipeline integrity. The data from the FEA analysis will allow for a better understanding of pipeline behavior in the presence of gouge defects and a more precise determination of burst pressure. This advancement could contribute to optimizing pipeline management, ensuring better safety, and reducing costs associated with repairs.

2.4.1. Numerical Model

A numerical model was developed using SolidWorks to simulate the behavior of a pipeline section, subjected to internal pressure and exhibiting a gouge defect. The study focuses on the API 5L X65 steel grade, with its mechanical and geometric properties detailed in Tables 3 and 4. The aim of this numerical model is to supersede traditional analytical expressions that derive burst pressure via circumferential and longitudinal stress, considering the morphology and orientation of the gouge defect.

Table 3. Mechanical properties of API 5L X65 steel tube [50]:

Mechanical properties	**Values**
Modulus of Elasticity, E	210 GPa
Poisson's ratio, ϑ	0,3
Yield Strength, σ_y	464 MPa
Ultimate tensile strength, σ_u	563 MPa
True ultimate tensile strength, σ_{uts}	629 MPa

Table 4. Geometric properties of API 5L X65 tube[50]:

Geometric properties	**Values**
Pipe outside diameter, D (mm)	250
Length of pipe, L (mm)	2000
Wall thickness, t (mm)	10

To reduce computation time without compromising the accuracy of the results, a reduced-size model was used in this study [51]. Furthermore, the pipe was specified with a length of 2,000 mm to avoid any influence of end conditions on the gouge defect areas during the finite element analysis. As this study focuses on single gouge defects (longitudinal, circumferential) with symmetrical geometries, only one quarter of the pipe was modeled (Figures 3 and 4) to accurately represent the actual geometry of the conduit.

2.4.2. Meshing and boundary conditions

To numerically model the burst pressure of pipelines with gouge defects, a tetrahedral solid mesh was generated in SolidWorks, using a curvature-based mesher for a high-quality mesh with 16 Jacobian points at the nodes. The mesh used, illustrated in Figure 5 (b), features refinement in the defect area. The theoretical burst pressure of the intact pipeline was quantified using Equation 5 [52]. Boundary conditions and mesh parameters were iteratively refined until a relative error of less than 5% was achieved between the theoretical and numerical burst pressure for the intact pipeline, as shown in Table 5. Further adjustments were made to the size and number of mesh elements, based on characteristic dimensions of the longitudinal and circumferential gouge defects, presented in Tables 6 and 7. This process improved the accuracy of burst pressure estimations while maintaining a conservative approach. The mesh is adapted to the specifics of each defect configuration. For the pipe with a longitudinal gouge, the maximum element size was 37.129 mm and the minimum size was 1.85645 mm, generating a high-quality mesh with 5820 nodes and 2895 elements, a maximum aspect ratio of 4.4182, and 66.5% of the elements having an aspect ratio less than 3 with no distortion. Conversely, for the pipe with a circumferential gouge, the maximum and minimum element sizes were 23.8688 mm and 1.19344 mm, respectively, with a "draft quality" mesh containing 1833 nodes and 5223 elements. The maximum aspect ratio was 3.5667 and 99.8% of the elements have an aspect ratio less than 3 with a percentage of distorted elements of 0%. This choice of parameters, including the tetrahedral mesh type, the mesher, and the element dimensions, is the result of an iterative process guided by the results of the study, the data in Tables 6 and 7, and the precision requirements, ensuring an accurate estimation of the burst pressure. The process allowed for the selection of an appropriate mesh for each configuration, as well as the boundary conditions, in order to obtain reliable estimates.

$$P_i = \frac{\sigma_{uts} . t}{r_i} \quad (5)$$

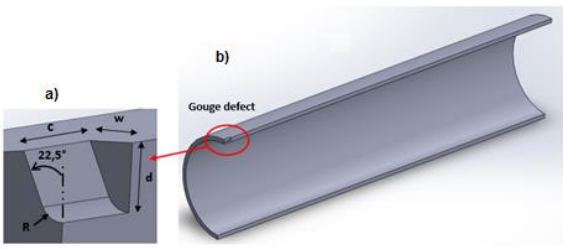

Figure 3. a) Geometry of the gouge defect;b) quarter of the tube infected by a gouge defect in longitudinal position.

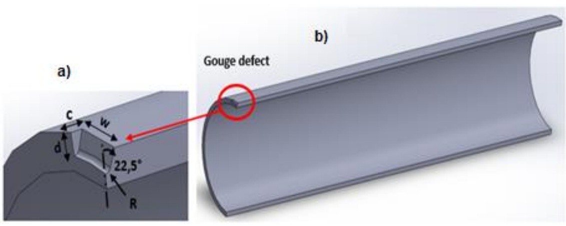

Figure 4. a) Geometry of the gouge defect;b) quarter of the tube infected by a gouge defect in circumferential position.

Table 5. Comparison between and theoretical numerical burst pressure for intact pipe API 5L X65:

Theoretical burst pressure	Numerical burst pressure	Relative error
54.7 MPa	52.45 MPa	4,11 %

To numerically simulate the burst pressure, the following boundary conditions were applied to a quarter model of the pipeline (Figure 5 (a)) in order to minimize computation time: a symmetry condition on face A, a fixed support (encastre) on edge B, internal pressurein C, and blocked displacement on the axes of the plane of face D. These conditions are applied to both models, with longitudinal and circumferential defects.

2.5. Failure Criterion

To further validate the finite element method, the results from this method were compared to results obtained using thin-walled pressure vessel theory. The results from the finite element method that are of interest to us are the maximum circumferential and longitudinal stresses. In the presence of the gouge defect, the finite element method should produce results close to those of theoretical calculations. The theoretical values of circumferential stress and longitudinal stress are determined using Equations 1through 4.

Burst failure of the pipe occurs when the local stress (axial or circumferential) in the defective area exceeds the limit criterion [53], in this case, the ultimate tensile strength $\sigma_{UTS}$of the material. Cylindrical coordinates were used in the numerical simulation to accurately estimate the maximum stress in the defective area [54].

2.6. Burst pressure by theoretical and numerical approach

Theoretical and numerical approaches were used to evaluate burst pressure. Theoretical calculations, employing Equations 3 and 4 for longitudinal ($P_{b\text{-theo-long}}$) and circumferential ($P_{b\text{-theo-circ}}$) gouge defects respectively, were validated by numerical simulations ($P_{b\text{-num-long}}$ and $P_{b\text{-num-circ}}$) using SolidWorks. These simulations, employing appropriate meshing and boundary conditions, aimed to match theoretical results, strengthening confidence in predictive methods, particularly for geometrically complex defects. The geometric parameters of the defect (length 2.c or width 2.w depending on the defect type, relative depth d/t, and relative width w/re) were considered in the theoretical approach. The parameter "q," representing the defect type and documented in Table 6 and 7, was arbitrarily chosen and used solely during the subsequent prediction of burst pressure via polynomial regression; its values distinguished longitudinal (1) from circumferential (0.1) gouges.

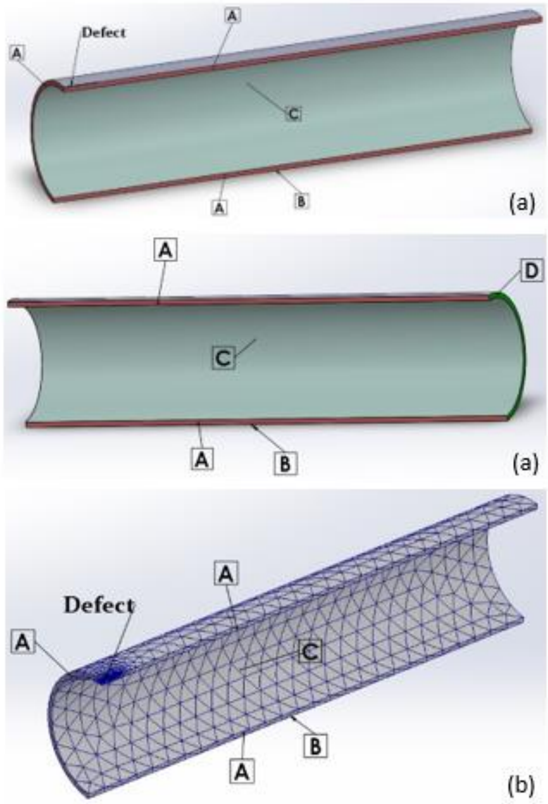

Figure 5. (a) Boundary conditions and loading; (b) Mesh.

Table 6. Burst pressures (theoretical and numerical) for longitudinal gouge.

2.c	d/t	q	w/r_e	$P_{b\text{-theo-long}}$	$P_{b\text{-num-long}}$	2.c	d/t	q	w/r_e	$P_{b\text{-theo-long}}$	$P_{b\text{-num-long}}$
40	0,1	1	0,32	44,687	42,75	40	0,4	1	0,32	37,723	35,95
60				43,959	42,45	60				34,805	35,43
80				43,489	41,58	80				33,105	34,87
100				43,174	40,4	100				32,038	34,25
120				42,952	39,87	120				31,317	34,02
140				42,789	39,5	140				30,802	33,74
160				42,663	38,7	160				30,416	33,23
180				42,565	38,55	180				30,119	32,65
200				42,486	38,35	200				29,881	31,95
220				42,420	38,05	220				29,689	30,12
40	0,2			42,715	40,82	40	0,5			34,497	33,15
60				41,247	40,15	60				30,940	32,75
80				40,327	39,6	80				28,957	30,52
100				39,722	38,85	100				27,744	29,34
120				39,302	38,65	120				26,938	28,43
140				38,995	38,45	140				26,369	28,12
160				38,762	38,05	160				25,947	27,75
180				38,579	37,78	180				25,623	27,49
200				38,433	36,17	200				25,366	27,66
220				38,313	35,65	220				25,158	25,9
40	0,3			40,422	38,88	40	0,6			30,575	29,92
60				38,216	38	60				26,521	26,47
80				36,879	37,45	80				24,375	24,68
100				36,020	36,12	100				23,100	24,57
120				35,430	35,85	120				22,268	24,08
140				35,004	34,75	140				21,688	23,31
160				34,683	33,95	160				21,261	22,04
180				34,434	33,35	180				20,936	21,64
200				34,234	32,95	200				20,679	21,4
220				34,071	32,12	220				20,472	21,03

Table 7. Burst pressures (theoretical and numerical) for circumferential gouge:

	d/t	q	w/r_e	$P_{b\text{-theo-circ}}$	$P_{b\text{-num-circ}}$	2.w	d/t	q	w/r_e	$P_{b\text{-theo-circ}}$	$P_{b\text{-num-circ}}$
40	0,1	0,1	0,32	89,612	97,45	40	0,4	0,1	0,32	77,481	82,47
60			0,48	88,151	96	60			0,48	71,509	78,05
80			0,64	86,810	93,15	80			0,64	66,494	72,15
100			0,8	85,605	90,47	100			0,8	62,318	66,98
120			0,96	84,549	88,53	120			0,96	58,877	62,08
140			1,12	83,652	87,5	140			1,12	56,084	60,23
160			1,28	82,919	85,9	160			1,28	53,866	55,18
180			1,44	82,351	84,3	180			1,44	52,166	53,36
200			1,6	81,948	83,45	200			1,6	50,938	52,86
220			1,76	81,705	82,65	220			1,76	50,147	51,74
40	0,2		0,32	86,076	90,45	40	0,5		0,32	72,032	78,5
60			0,48	83,124	89,8	60			0,48	64,598	70,03
80			0,64	80,481	88,15	80			0,64	58,612	63,75
100			0,8	78,159	85,46	100			0,8	53,792	58,2
120			0,96	76,161	82,1	120			0,96	49,923	53,15
140			1,12	74,486	79,63	140			1,12	46,842	49,63
160			1,28	73,129	75,8	160			1,28	44,424	46,8
180			1,44	72,081	71,12	180			1,44	42,577	39,26
200			1,6	71,333	69,75	200			1,6	41,234	38,7
220			1,76	70,873	65,72	220			1,76	40,348	37,55
40	0,3		0,32	82,084	88,47	40	0,6		0,32	65,361	70,68
60			0,48	77,622	84,78	60			0,48	56,611	60,1
80			0,64	73,741	81,47	80			0,64	49,920	53,4
100			0,8	70,415	77,23	100			0,8	44,743	48,53
120			0,96	67,612	72,85	120			0,96	40,711	43,33
140			1,12	65,297	68,74	140			1,12	37,567	40,8
160			1,28	63,440	65,25	160			1,28	35,132	37,48
180			1,44	62,011	63,42	180			1,44	33,280	35,95
200			1,6	60,985	61,78	200			1,6	31,923	34,4
220			1,76	60,339	59,32	220			1,76	31,004	33,2

Figure6.(a) and 6.(b) demonstrate a strong positive correlation between the numerical ($P_{b\text{-}num}$) and theoretical ($P_{b\text{-}theo}$) burst pressures for longitudinal and circumferential defects, respectively. The majority of the numerical results fall within a ±10% margin of the theoretical values, thus validating the accuracy of the numerical approach. The observed trend is that the numerical approach provides a conservative estimate of the burst pressure, even in the rare cases of higher error. This confirms the reliability and conservative nature of the numerical modeling for predicting the behavior of gouge defects in pipelines.

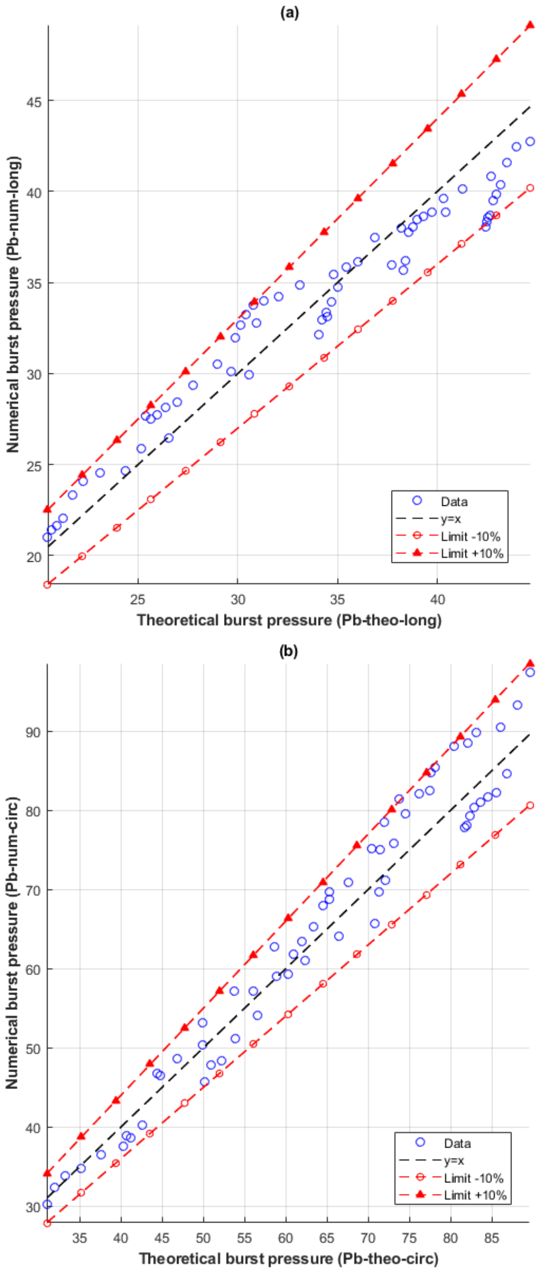

Figure 6. Relative error on burst pressure with ±10% limits.

This satisfactory performance inspires confidence in the validity of the numerical approach as a robust tool for predicting burst pressure within the limits of the parameters studied. This validation confirms that the numerical models developed in SolidWorks, using appropriate boundary conditions and mesh, are capable of simulating the burst phenomenon with acceptable accuracy. The results obtained demonstrate the effectiveness of this method for evaluating the strength of mechanical structures and can be used with confidence for design analyses and optimizations. In summary, although the numerical models generally reproduce the theoretical trend of burst pressure, a quantitative study of the errors is necessary to better characterize overall performance.

2.7. Flowchart for Optimal Burst Pressure Prediction via a Polynomial Equation

The flowchart in Figure 7 details a MATLAB implementation of polynomial regression (a regression-based predictive modeling technique implemented in a machine learning workflow) to model the non-linear relationship between defect characteristics (length 2c or width 2w, d/t ratio, defect type q and the w/r_e ratio) and burst pressure. It begins with loading the data, separating it into features (X) and target variable (y), dividing it into training and testing sets (80/20), and standardizing these sets.

We chose an 80% training and 20% testing split after comparing model performance across various proportions, as clearly illustrated in our Table 8. Our key observations were as follows:

- 70/30 Split: Allocating 70% of the data for training would have potentially limited our model's ability to capture all the nuances and complexity inherent in the data. The risk was a less "faithful" model with reduced generalization performance, even if a larger test set might have offered a robust validation of the observed performance.
- 90/10 Split: Conversely, a 90/10 split would certainly have provided the model with a very large volume of data for training. However, such a small test set (10% of the data) might not have sufficiently represented the overall data variability. Performance observed on such a restricted sample wouldn't reliably confirm the model's true accuracy and robustness across a broader range of real-world scenarios, running the risk of overestimating its capabilities.

Ultimately, the 80/20 split proved to be the ideal compromise for our study. This balance allowed us to provide the model with enough training data to properly understand complex relationships (especially interactions between defect parameters), while ensuring a substantial enough test set (20%) for a reliable and statistically significant evaluation of its performance and generalization ability. This balance is precisely what led us to the high coefficients of determination (R^2) and very low Root Mean Square Error (RMSE) that we present in the article.

Next, the code explores a space of polynomial models. For each combination of polynomial degree (from 1 to 5) and presence/absence of interaction terms, it creates new polynomial features and trains a polynomial regression model using the normal equation: $\theta = (X^TX)^{-1}X^Ty$. In this equation, θ represents the parameter vector (theta), X is the design matrix (polynomial and interaction features), y is the target variable vector, X^T is the transpose of X, and $(X^TX)^{-1}$ is the inverse of (X^TX). The normal equation directly calculates the parameter values (θ) using only the design matrix (X) and the target variable vector (y) from the training set.

The code evaluates each model using its θ parameters to make predictions on the training and testing sets and calculating the R^2 and RMSE metrics. The retained polynomial configuration is the one that maximizes performance on the test set (RMSE<1, R^2>0.99), while controlling for overfitting by examining performance on the training set. The results include the metrics, their graphs, the polynomial equation, and the correlation coefficients (r), to characterize the final model. The process aims to capture the relationships between the defects and burst pressure.

Table 8. Impact of data distribution on model accuracy

Data distribution (Train/Test)	Polynomial structure	R^2		RMSE	
		(train set)	(test set)	(train set)	(test set)
70/30	Degree: 1, Without interactions	0.874	0.901	6.841	7.451
	Degree: 1, With interactions: 1	0.729	0.689	7.523	6.251
	Degree: 2, Without interactions	0.941	0.841	4.61	5.826
	Degree: 2, With interactions: 1	0.982	0.95	3.362	2.839
80/20	Degree: 1, Without interactions	0.948	0.926	4.55	5.104
	Degree: 1, With interactions: 1	0.996	0.997	1.1	1.096
	Degree: 2, Without interactions	0.954	0.934	4.269	4.804
	Degree: 2, With interactions: 1	0.998	0.997	0.888	0.936
90/10	Degree: 1, Without interactions	0.951	0.872	3.21	6.142
	Degree: 1, With interactions: 1	0.986	0.908	1.02	3.623
	Degree: 2, Without interactions	0.989	0.915	2.89	2.74
	Degree: 2, With interactions: 1	0.997	0.956	0.973	1.465

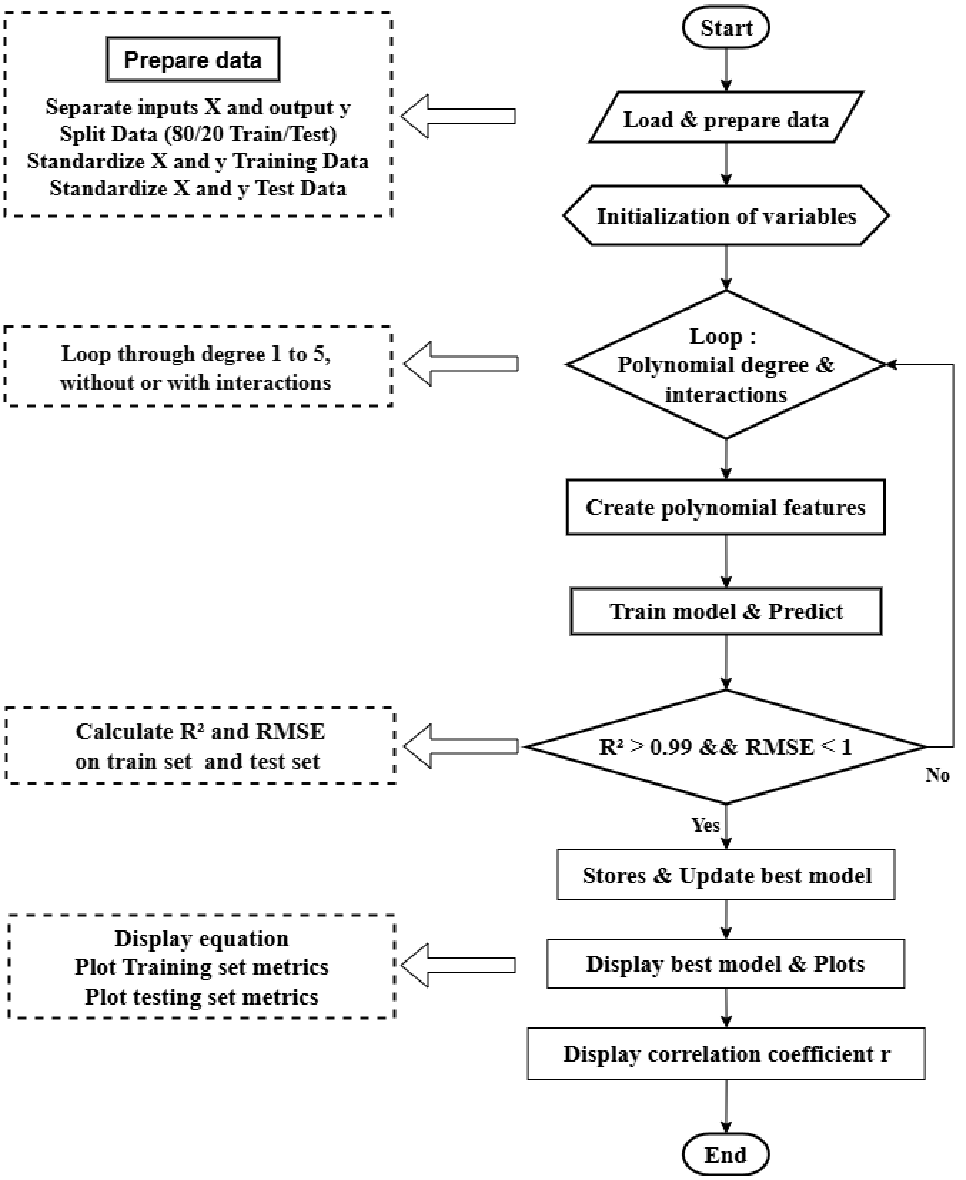

Figure 7. Steps for burst pressure prediction via a polynomial model implemented in MATLAB.

2.8. Polynomial regression equation

Polynomial regression, like many Machine Learning (ML) algorithms, is sensitive to the scale of input variables. In other words, the range of values for different variables can affect the performance of the algorithm. If some variables have very large values (for example, the length or width of the defect) while others have smaller values (for example, the d/t ratio, the defect type q and the w/re ratio), the algorithm might unintentionally give more weight to the variables with high magnitude. This distortion, induced by scale differences, risks producing suboptimal regression coefficients and, consequently, degraded model performance. To avoid this problem, data standardization is crucial. By putting all variables on a comparable scale (for example, by centering and reducing the data), we ensure that the algorithm treats each variable fairly, which leads to more accurate regression coefficients and better overall model performance [55].

2.8.1. Prediction of burst pressure

For burst pressure prediction, we used polynomial regression with interactions, implemented in MATLAB R19a. Standardization (z-score) was applied to the input data, ensuring a mean of 0 and a standard deviation of 1 (Equation 6). The learning process consisted of building polynomial regression models (degree 1 to 5, with or without interactions), generating polynomial and interaction features. The optimal coefficients were estimated by the normal equation of linear regression, minimizing the error on the training data. Model performance (R^2 and RMSE) was evaluated on the test set. The selected model was the one with the lowest possible degree, with an R^2 greater than 0.99 and an RMSE less than 1 on the test data. Finally, burst pressure prediction was obtained by using the polynomial equation (with its optimized coefficients) on the standardized input data.

$$z = \frac{x - \mu}{\sigma} \tag{6}$$

The results in Table 9 show that interactions between variables are essential for good prediction. Models that do not take these interactions into account have unsatisfactory performance. Adding interactions, whether it is a first-order or second-order model, significantly improves predictions, with a slight advantage for the second-order model.

Table 9. Results of evaluation metrics for different polynomial regression models:

Polynomial structure	R^2		RMSE	
	(train)	(test)	(train)	(test)
Degree: 1, Without interactions	0.948	0.926	4.55	5.104
Degree: 1, With interactions: 1	0.996	0.997	1.1	1.096
Degree: 2, Without interactions	0.954	0.934	4.269	4.804
Degree: 2, With interactions: 1	0.998	0.997	0.888	0.936

2.8.2. Polynomial regression model

The analysis of the results reveals that polynomial models with interactions offer superior performance compared to those without interactions, starting as early as degree 1. Although the degree 1 model with interactions achieves acceptable performance (R^2 of 0.997 and RMSE of 1.096 on the test set), the degree 2 model with interactions presents a significant improvement with an R^2 of 0.997 and an RMSE of 0.936 on the test, thus satisfying our performance criteria ($R^2 > 0.99$ and RMSE < 1). Despite a slightly increased complexity, the improved performance justifies the choice of the polynomial model of degree 2 with interactions for enhanced prediction accuracy.

The form of the polynomial equation for a degree 2 model with interactions [56]is written as:

$$y_{pred} = a_0 + \sum_{i=1}^{n} a_i.x_i + \sum_{j=1}^{n} b_j.x_j^2 + \sum_{i=1}^{n}\sum_{j=i+1}^{n} c_{ij}.x_i.x_j \tag{7}$$

- a_0 is the y-intercept.
- $\sum_{i=1}^{n} a_i.x_i$: Represents the linear effects of the variables xi.
- $\sum_{j=1}^{n} b_j.x_j^2$: Represents quadratic terms (degree 2).
- $\sum_{i=1}^{n}\sum_{j=i+1}^{n} c_{ij}.x_i.x_j$: Models the interactions between two variables.
- Standardized output equation (burst pressure):

$$\begin{aligned} y_{pred\_z} = {} & -0.0815 - 0.2475.x_{1z} \\ & - 0.5149.x_{2z} \\ & - 0.2129.x_{3z} \\ & + 0.7218.x_{4z} \\ & + 0.0472.x_{1z}^2 \\ & - 0.0192.x_{2z}^2 \\ & + 0.5204.x_{3z}^2 \\ & - 0.0115.x_{4z}^2 \\ & - 0.0366.x_{1z}.x_{2z} \\ & + 0.2077.x_{1z}.x_{3z} \\ & + 0.0871.x_{1z}.x_{4z} \\ & + 0.1063.x_{2z}.x_{3z} \\ & - 0.1024.x_{2z}.x_{4z} \\ & + 0.7053.x_{3z}.x_{4z} \end{aligned} \tag{8}$$

- Unstandardized output equation:

After prediction, unstandardized equation is applied to bring the results back to the original scale because the model was trained on standardized (centered-reduced) data. This step, essential for interpretation, uses Eq. 9 to convert the standardized prediction y_{predz} into y_{pred}, which is expressed in the same units as the target data. This allows for a relevant evaluation of the model's performance.

$$y_{pred} = y_{pred_z}.\sigma_{y\_train} + \bar{y}_{train} \tag{9}$$

With:

$\sigma_{y\_train} = 20{,}094$ MPa

$\bar{y}_{train} = 49{,}12$ MPa

3. Results and Discussion

3.1. Burst pressure by numerical approach

The boxplots in Figure8 reveal distinct characteristics for the relative errors of longitudinal and circumferential gouge defects. For both types of defects, the medians of relative errors are very close to 0%, indicating a general accuracy of the model. The interquartile range (IQR) is approximately between -6% and +4% in both cases, highlighting a similar dispersion of errors around the median. However, the extreme errors (whiskers) indicate a slight difference: for the longitudinal defect, the errors extend to approximately ±10%, while for the circumferential defect, the errors range from -10% to +9%.Despite these minor differences, the numerical approach is validated for both types of defects, with overall accuracy and similarity in the dispersion of errors.

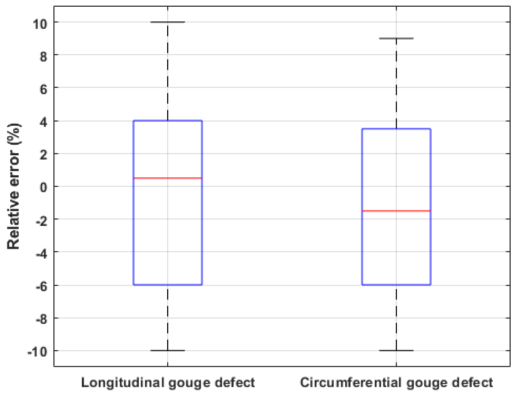

Figure 8. Boxplot of relative errors for longitudinal and circumferential gouges.

3.2. Burst pressure prediction by machine learning (polynomial regression)

Both graphs (a) and (b) in Figure 9 consistently show that the addition of interactions between variables has a massive impact on the performance of the model. Models without interactions (degree 1 or 2) have poor performance, with a high RMSE and a low R^2, while models with interactions have a low RMSE and a high R^2, which is significantly better. Adding polynomial terms of degree 2 without interactions does not result in improved model performance, suggesting that the data does not exhibit strong non-linearity apart from the interactions. The polynomial degree is not a key element in improving performance. It is concluded that interactions play a leading role in the model's ability to represent the training data.

The graphs in Figure 10 clearly show that adding interactions is essential to achieving good generalization of the model to new data. The behavior is identical on the training set and on the test set. The trends observed on the test set are very similar to those observed on the training set:

- Interactions are key.
- Increasing the degree without interaction is useless.
- The model with interactions (degree 1 or 2) has the best performance.

This similarity reinforces confidence in the validity of the model.

Figure 11 shows the relationship between predicted values and actual values for training and testing. We observe the following:

- Training Set:
  - The training graph displays a very high r coefficient of 0.999. This indicates a near-perfect linear correlation between the model's predictions and the actual target values in the training set.
  - The data points are clustered very tightly around the blue fit line, with an equation of the fit line being ypred-train ~= ytrain + 0.097. The slope is approximately 1, which means that the predicted value is almost equal to the actual target value. This implies that the model has learned the training data very well and can accurately predict the outputs based on the training's input features.
- Test Set:
  - The test graph also presents a very high r coefficient of 0.998. This reveals a strong linear correlation between the model's predictions and the actual target values in the test set.
  - The data points are clustered tightly around the green fit line. The equation of the fit line is ypred-test ~= 0.99*ytest+ 0.56, and the slope is approximately 0.99.
  - This demonstrates that the model is not only accurate but has also generalized well, meaning it can make reliable predictions on new data it hasn't seen during training. The very high R correlation coefficient on the test indicates that the model's performance remains excellent on the test set, which is desirable.

In summary, the similarity of the r coefficients on the training and test sets is a good indicator of the model's performance. This indicates that the model has been able to learn the relationships between the features and the target and to generalize its knowledge to make good predictions on new data. The slight difference between the r coefficient values suggests that there might be a slightly larger fit on the training, but this remains very acceptable and is an ideal situation.

The polynomial regression equation we developed represents a directly applicable tool for industry. Its formal simplicity and high accuracy make it a major asset. Practically, if implemented in a mobile application or computer software, this equation will enable engineers and technicians to instantly obtain a reliable estimate of the burst pressure for a pipeline with a gouge defect. Whether directly in the field during an inspection, or in a control room for in-depth analysis, this tool will greatly facilitate quick and informed decision-making regarding the pipeline's fitness-for-service and the maintenance measures to consider. This marks a significant advance towards proactive and secure infrastructure integrity management.

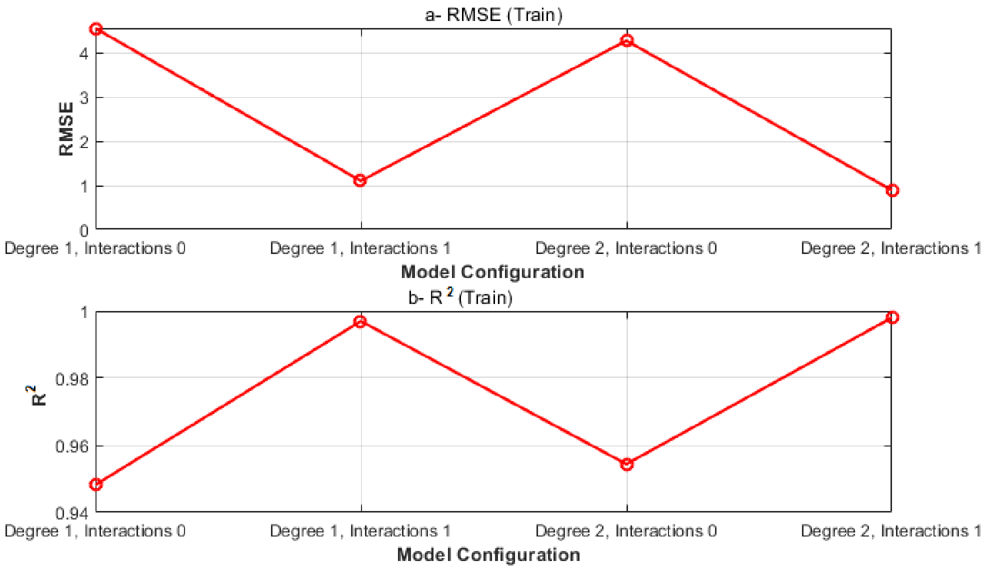

Figure 9. Performance metrics (Training) by model configuration.

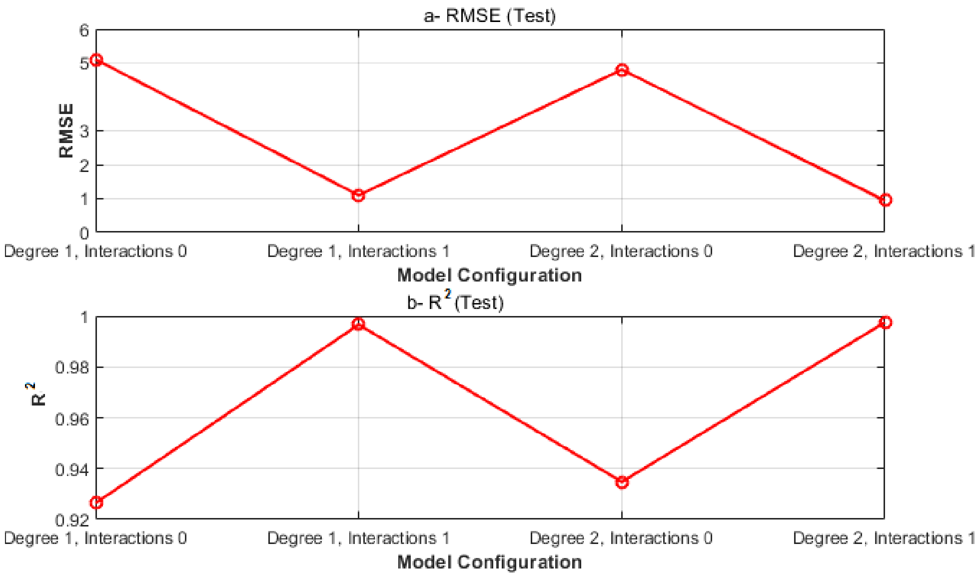

Figure 10. Performance metrics (Testing) by model configuration.

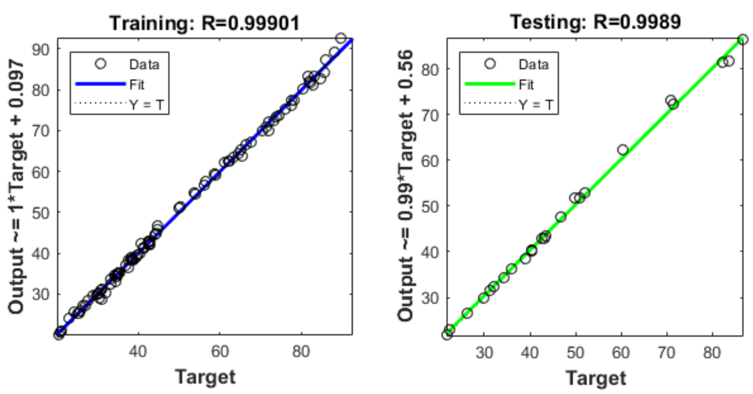

Figure 11. Prediction performance (Training and Testing).

3.3. Burst Pressure (Simulation vs. Prediction)

The evaluation of the numerical and predictive approaches was carried out by comparing their estimates to the values of the theoretical approach (Figure 12), focusing on the average relative errors, with the following values:

Table 10. Relative errors of the numerical vs. predictive approach:

	Relative errors (%)	
	Numerical approach	Predictive approach
Longitudinal gouge	5	1
Circumferential gouge	5	2

These figures clearly show that, for both types of defects, the predictive approach ($P_{b\text{-pred-long}}$and $P_{b\text{-pred-circ}}$) is more accurate than the numerical model ($P_{b\text{-num-long}}$and $P_{b\text{-num-circ}}$). Indeed, the average relative errors of the predictive approach are considerably lower than those of the numerical approach. The predictive approach reduces the relative error from 5% to only 1% in the case of the longitudinal defect and from 5% to 2% in the case of the circumferential defect (Table 10). In conclusion, given these comparatively lower average relative errors and how the predictive curves follow the theoretical curves, the predicted pressure method more faithfully models the semi-empirical equations than the numerical method for both types of defects. This reinforces the predictive approach as being more accurate for estimating burst pressure in the context studied.

3.4. Assessment of the severity of gouge defects

The quantitative analysis of pipeline burst pressure data from Figure 13 highlights a predominant influence of the relative defect depth (d/t). Maintaining the length or width (2c or 2w) constant at 40 mm, the burst pressure for a longitudinal defect (Pb_theo_long) decreases significantly with increasing d/t. Specifically, Pb_theo_longdrops from 44,69 MPa (for d/t = 0,1) to 30,58 MPa (for d/t = 0,6). This variation of 14,11 MPa represents a significant reduction of 31,57% in the pipeline's ability to withstand internal pressure, demonstrating the critical impact of defect depth.

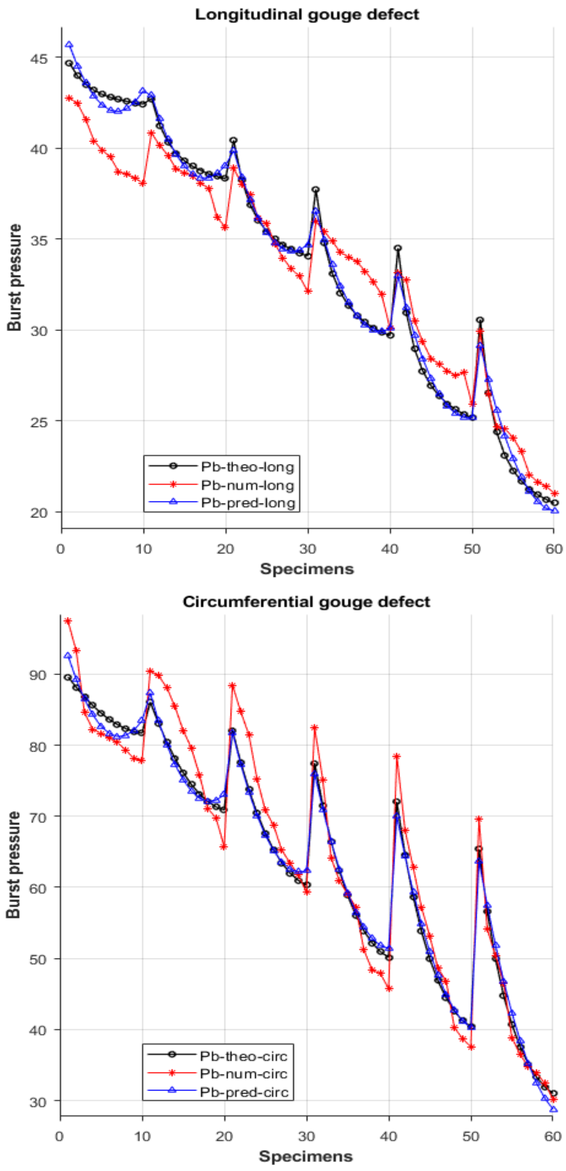

Figure 12. Burst Pressure Comparison: Numerical vs Predicted.

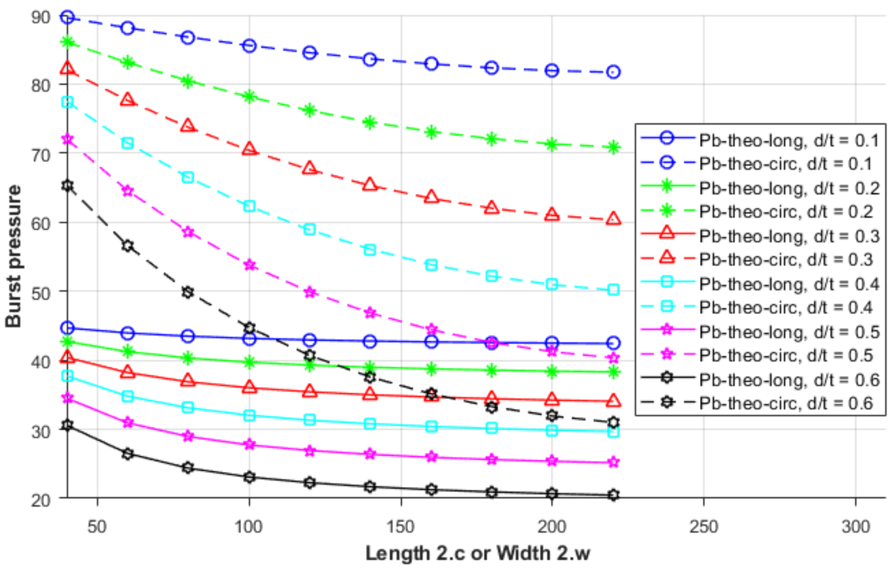

Figure 13. Theoretical Longitudinal vs. Circumferential Burst Pressure.

Furthermore, the analysis confirms that longitudinal defects pose a higher risk than circumferential defects. At a defect length of 2c = 60 mm and for a relative depth of 0,3, $P_{b_theo_long}$is evaluated at 38,22 MPa, while $P_{b_theo_circ}$reaches 77,622 MPa when the defect width 2w also corresponds to 60 mm. The burst pressure for the circumferential defect is therefore approximately twice that of the longitudinal defect, highlighting the increased vulnerability of pipelines with longitudinal defects. This observation emphasizes the need for particular attention during inspections and maintenance programs. While the influence of defect length or width (2c or 2w) is secondary compared to that of d/t, it also contributes to the reduction of burst pressure. This trend can be observed by analyzing the variation of $P_{b_theo_circ}$with the width (2w).

A crucial aspect revealed by the analysis is the presence of overlapping zones between the curves. These overlaps indicate that a circumferential defect with a high relative depth can exhibit a burst pressure similar to that of a longitudinal defect with a lower relative depth. For example, a circumferential defect with d/t = 0,5 and 2w = 200 mm could have a burst pressure of around 40 MPa, a value comparable to that of a longitudinal defect with d/t = 0.3 and 2c = 60 mm. This observation underscores that depth alone is insufficient for evaluating pipeline pressure, but rather the interaction between defect depth, its dimension, and its type must be considered. Therefore, the combination of all these factors must be taken into account. The prioritization of inspections and maintenance interventions should be guided by this quantitative analysis, paying particular attention to deep longitudinal defects, in order to ensure the safety and reliability of pipelines.

4. Conclusion

This study successfully developed a novel burst pressure prediction equation for API 5L X65 pipelines affected by both longitudinal and circumferential gouge defects. Our key contribution directly addresses a significant gap in the literature: while machine learning is increasingly applied to corrosion defects, its use for predicting burst pressure in critical gouge defects has been almost non-existent until now. We deliberately chose polynomial regression, valuing its ability to provide an explicit and highly interpretable formula, which was essential for capturing the complex interactions among defect depth, length, and width. Initially, our theoretical approach was validated through numerical analyses, which then formed a reliable foundation for training our Machine Learning model.

Our polynomial regression model demonstrated

exceptional performance, achieving a near-perfect correlation (R^2 = 0.999 in training, 0.998 in testing). It also outperformed traditional numerical approaches, reducing the average relative error from 5% to just 1% for longitudinal defects and 2% for circumferential ones. This precision, coupled with the interpretability of our equation, unlocks major practical opportunities for the industry. Concretely: once integrated into a mobile application or computer software, our equation could empower engineers and technicians to instantly obtain reliable burst pressure estimations for a damaged pipeline. Whether directly in the field during an inspection, or in a control room for in-depth analysis, this ability to quickly and accurately assess pipeline integrity by highlighting the criticality of defect depth (especially for longitudinal gouges) and the necessity of considering defect orientation and interactions (as illustrated by overlapping curves) will facilitate proactive decision-making and optimize risk-based maintenance strategies.

However, while our model is robust and precise, it currently relies on data derived from numerical simulations, which constitutes a notable limitation in the absence of direct experimental validation. To strengthen these findings and broaden the scope of our work, several avenues for future research emerge. Crucially, future efforts should prioritize rigorous experimental validation to confirm the model's robustness under real-world conditions. Integrating new parameters such as residual stresses or fatigue, along with exploring a wider range of conditions, would further refine our predictions. Finally, a comparative study with other machine learning techniques, such as ANFIS, could uncover further improvements, thereby contributing to the continuous enhancement of safety and efficiency in energy infrastructure management.

References

[1] A. Cosham and P. Hopkins, “An Overview of the Pipeline Defect Assessment Manual,” 4th International Pipeline Conference, vol. 44, no. May, pp. 1–13, 2004.

[2] O. Obeid, G. Alfano, H. Bahai, and H. Jouhara, “Mechanical response of a lined pipe under dynamic impact,” Engineering Failure Analysis, vol. 88, pp. 35–53, 2018. https://doi.org/10.1016/j.engfailanal.2018.02.013

[3] Z. Mighouar, H. Khatib, L. Zahiri, and K. Mansouri, “A Classification and Comparison of Crack and Dent Defects in a Metal Pipe Subjected to Variable Amplitude Loading,” International Journal of Automotive and Mechanical Engineering, vol. 19, no. 1, pp. 9577–9592, 2022. https://doi.org/10.15282/ijame.19.1.2022.20.0739.

[4] British Standards Institution, “BSI Standards Publication Guide to methods for assessing the acceptability of flaws in metallic structures,” BSI Stand. Publ., no. UK, p. 490, 2019.

[5] K. J. Yeom, Y. K. Lee, K. H. Oh, C. M. Kim, and W. S. Kim, “Integrity assessment of API 5L X65 and X70 pipelines with mechanical damages,” in International Pipeline Conference, American Society of Mechanical Engineers, 2012, pp. 603–609. https://doi.org/10.1115/IPC2012-90017.

[6] D. Oh, J. Race, S. Oterkus, and B. Koo, “Burst pressure prediction of API 5L X-grade dented pipelines using deep neural network,” Journal of Marine Science and Engineering, vol. 8, no. 10, p. 766, 2020. https://doi.org/10.3390/jmse8100766.

[7] H. Zhao, X. Liang, Z. Yang, P. He, and B. Zhao, “Experimental and Numerical Analysis of the Impact of Corrosion on the Failure Pressure of API 5L X65 Pipeline,” Journal of Marine Science and Engineering., vol. 12, no. 10, 2024, https://doi.org/10.3390/jmse12101810.

[8] L. Zahiri, H. Khatib, M. E. Ech-Chhibat, M. Jammoukh, Z. Mighouar, And K. Mansouri, “Numerical Analysis Of The Harmfulness Of The Fatigue-Corrosion Defect In A Metal Pipe Under Internal Pressure,” International Journal of Emerging Trends in Engineering Research, vol. 8, no. 10, 2020. https://doi.org/10.30534/ijeter/2020/528102020.

[9] A. S. Ameed, F. M. Mohammed, and A. L. Shuraiji, “Effect of Laser Surface Treatment On the Crack Growth of Al-6061 Alloy Under Impact Dynamic Load.,” Jordan Journal of Mechanical & Industrial Engineering, vol. 18, no. 3, 2024. https://doi.org/10.59038/jjmie/180307.

[10]H. Gholami, S. Shahrooi, and M. Shishesaz, "Predicting the Burst Pressure of High-Strength Carbon Steel Pipe with Gouge Flaws Using Artificial Neural Network," Journal of Pipeline Systems Engineering and Practice, vol. 11, no. 4, pp. 1–9, 2020, doi: 10.1061/(asce)ps.1949-1204.0000478. https://doi.org/10.1061/(ASCE)PS.1949-1204.0000478.

[11] N. A. Alang, N. A. Razak, K. A. Shafie, and A. Sulaiman, "Finite element analysis on burst pressure of steel pipes with corrosion defects," in 13th International conference on fracture, 2013, pp. 1–10.

[12] H. Liu, F. Khan, and P. Thodi, "Revised burst model for pipeline integrity assessment," Engineering Failure Analysis, vol. 80, no. May, pp. 24–38, 2017, https://doi.org/10.1016/j.engfailanal.2017.01.018.

[13] X. K. Zhu and B. N. Leis, "Evaluation of burst pressure prediction models for line pipes," International Journal of Pressure Vessels and Piping, vol. 89, pp. 85–97, 2012, doi: 10.1016/j.ijpvp.2011.09.007. https://doi.org/10.1016/j.ijpvp.2011.09.007.

[14] A. Rachman, T. Zhang, and R. M. C. Ratnayake, "Applications of machine learning in pipeline integrity management: A state-of-the-art review," International Journal of Pressure Vessels and Piping, vol. 193, p. 104471, 2021, https://doi.org/10.1016/j.ijpvp.2021.104471.

[15] C. T. Belachew, M. C. Ismail, and S. Karuppanan, "Burst strength analysis of corroded pipelines by finite element method," Journal of Applied Sciences, vol. 11, no. 10, pp. 1845–1850, 2011. DOI: 10.3923/jas.2011.1845.1850.

[16] U. Sarwar et al., "Enhancing pipeline integrity: a comprehensive review of deep learning-enabled finite element analysis for stress corrosion cracking prediction," Engineering Applications of Computational Fluid Mechanics, vol. 18, no. 1, p. 2302906, 2024. https://doi.org/10.1080/19942060.2024.2302906.

[17] P. Zhao, J. Shuai, M. Sun, Z. Lv, K. Xu, and Y. Wang, "Burst pressure of thin-walled pipes with dent and gouge defects," Thin-Walled Struct., vol. 159, no. November 2020, p. 107213, 2021, https://doi.org/10.1016/j.tws.2020.107213.

[18] S. Republic, G. N. Ireland, N. Gas, C. Republic, and O. G. Europe, "Gas pipeline incidents 12," no. September 2023, 2022.

[19] J. Kiefner, W. Maxey, R. Eiber, and A. Duffy, "Failure stress levels of flaws in pressurized cylinders," in Progress in flaw growth and fracture toughness testing, ASTM International, 1973. https://doi.org/10.1520/STP49657S

[20] HOPKINS,P., CORBIN,P.; A Study of External Damage of Pipelines, Paper 5, NG18/EPRG Seventh Joint Biennial Technical Meeting on Line Pipe Research, Calgary, Alberta, Canada, 29 August - 1 September 1988.

[21] A. G. Miller, "Review of limit loads of structures containing defects," International Journal of Pressure Vessels and Piping, vol. 32, no. 1–4, pp. 197–327, 1988.

[22] P. Roovers, M. R. Galli, R. J. Bood, U. Marewski, M. Steiner, and M. Zarea, "Eprg methods for assessing the tolerance and resistance of pipelines to external damage. Pt. 1," 3R. Rohre, Rohrleitungsbau, Rohrleitungstransport, vol. 38, 1999.

[23] M. Lo, S. Karuppanan, and M. Ovinis, "ANN-and FEA-based assessment equation for a corroded pipeline with a single corrosion defect," Journal of Marine Science and Engineering, vol. 10, no. 4, p. 476, 2022. https://doi.org/10.3390/jmse10040476.

[24] T. Arumugam, S. Karuppanan, and M. Ovinis, "Materials Today : Proceedings Residual strength analysis of pipeline with circumferential groove corrosion subjected to internal pressure," Materials Today: Proceedings, vol. 29, no. November 2018, pp. 88–93, 2020, doi: 10.1016/j.matpr.2020.05.699. https://doi.org/10.1016/j.matpr.2020.05.699.

[25] T. Arumugam, S. Karuppanan, and M. Ovinis, "Finite element analyses of corroded pipeline with single defect subjected to internal pressure and axial compressive stress," Marine Structures, vol. 72, p. 102746, 2020. https://doi.org/10.1016/j.marstruc.2020.102746

[26] W. Xu, C. Bao, J. Choung, and J. Lee, "Corroded pipeline failure analysis using artificial neural network," Advances in Engineering Software, vol. 0, pp. 1–12, 2017, https://doi.org/10.1016/j.advengsoft.2017.05.006.

[27] S. Devi, V. Kumar, S. Karuppanan, and M. Ovinis, "Artificial Neural Network-Based Failure Pressure Prediction of API 5L X80 Pipeline with Circumferentially Aligned Interacting Corrosion Defects Subjected to Combined Loadings," Materials 2022, 15, 2259 https://doi.org/10.3390/ma15062259.

[28] K. A. Macdonald and A. Cosham, "Best practice for the assessment of defects in pipelines - Gouges and dents," Eng. Fail. Anal., vol. 12, no. 5 SPEC. ISS., pp. 720–745, 2005, doi: 10.1016/j.engfailanal.2004.12.011..

[29] J. H. Panchal, M. Fuge, Y. Liu, S. Missoum, and C. Tucker, "Machine learning for engineering design," Journal of Mechanical Design, vol. 141, no. 11, p. 110301, 2019. https://doi.org/10.1115/1.4044690.

[30] Y. El Kiri, L. Zahiri, K. Mansouri, Z. Mighouar, and S. El Ouardi, "Prediction of the rupture pressure of a corroded pipeline by ANN," in E3S Web of Conferences, EDP Sciences, 2023, p. 31. https://doi.org/10.1051/e3sconf/202346900031.

[31] Y. El Kiri, Z. Mighouar, L. Zahiri, K. Mansouri, S. El Ouardi, and H. Chaiti, "Predicting the failure of plain dent pipeline subjected to cyclic loads using an artificial neural network," in 2023 7th IEEE Congress on Information Science and Technology (CiSt), IEEE, 2023, pp. 179–186. DOI: 10.1109/CiSt56084.2023.10409983.

[32] Y. El Kiria, L. Zahirib, K. Mansouric, and Z. Mighouard, "Assessment of the harmfulness of corrosion defects in a pressurized pipeline with a single corrosion defect using FEA and ANN," 2025. http://dx.doi.org/10.17515/resm2025-502ml1026rs.

[33] U. Graphene, A. Nanofluids, and L. K. G. Bhatta, "Radial basis Neural Network Model to Prediction of Thermal Resistance and Heat Transfer Coefficient of Oscillating Heat Pipe Using Graphene and Acetone-Based Nanofluids," Jordan Journal of Mechanical and Industrial Engineering, vol. 1, no. 2, pp. 251–266, 2024. https://doi.org/10.59038/jjmie/180201.

[34] Aleksandar Peckov, "A Machine Learning Approach to Polynomial Regression," Work, p. 156, 2012.

[35] R.-C. Wu, Y.-W. Tseng, and C.-Y. Chen, "Estimating parameters of the induction machine by the polynomial regression," Applied Sciences, vol. 8, no. 7, p. 1073, 2018. https://doi.org/10.3390/app8071073.

[36] A. M. S. Ragab, M. S. Yakoot, and O. Mahmoud, "Application of machine learning algorithms for managing well integrity in gas lift wells," in SPE Asia Pacific Oil and Gas Conference and Exhibition, SPE, 2021, p. D012S032R003. https://doi.org/10.2118/205736-MS.

[37] S. Per Håkon Jøranli, "Use of Machine Learning Techniques for Risk Based Inspection and Integrity Management of Pipeline Systems," 2019. [Online]. Available: http://hdl.handle.net/11250/2621110.

[38] A. F.O., A. R. O., and U. F. O., "Advancements in Machine Learning for Pipeline Integrity Management: A Comprehensive Review of Predictive and Optimization Techniques," Cognizance Journal of Multidisciplinary Studies, vol. 4, no. 11, pp. 129–138, 2024, doi: 10.47760/cognizance.2024.v04i11.011.

[39] R. Chen, Q. Wang, and A. Javanmardi, "A Review of the Application of Machine Learning for Pipeline Integrity Predictive Analysis in Water Distribution Networks," Archives of Computational Methods in Engineering , vol. 32, no. 6, pp. 3821–3849, 2025, doi: 10.1007/s11831-025-10251-6.

[40] M. Hussain, T. Zhang, I. Jamil, A. A. Soomro, and I. Hussain, "Application of machine learning approaches to prediction of

corrosion defects in energy pipelines," Advances in Corrosion Modelling, pp. 127–166, 2024. DOI:10.1007/978-3-031-60358-7_7.
[41] B. Cui, H. Wang, and X. Yang, "Artificial Intelligence-Enabled Pipeline Integrity Management for Detection and Prediction of Corrosion Defects," in Pipelines 2025, pp. 207–217. https://doi.org/10.1061/9780784486382.023.
[42] Z. He and W. Zhou, "Machine Learning Tools to Predict the Burst Capacity of Pipelines Containing Dent-Gouges," in International Pipeline Conference, American Society of Mechanical Engineers, 2022, p. V002T03A058. https://doi .org/10.1115/IPC2022-87176.
[43] H. C. Phan and A. S. Dhar, "Predicting pipeline burst pressures with machine learning models," International Journal of Pressure Vessels and Piping, vol. 191, no. March, p. 104384, 2021, doi: 10.1016/j.ijpvp.2021.104384. https://doi.org/ 10.1016/j.ijpvp.2021.104384.
[44] K. F. Tee and A. H. Wordu, "Burst strength analysis of pressurized steel pipelines with corrosion and gouge defects," Engineering Failure Analysis, vol. 108, p. 104347, 2020. https://doi.org/10.1016/j.engfailanal.2019.104347.
[45] A. Cosham and P. Hopkins, "The pipeline defect assessment manual," in International Pipeline Conference, 2002, pp. 1565–1581. https://doi.org/10.1115/IPC2002-27067.
[46] V. Vincenzo, "Circular Cylinders and Pressure Vessels," 2014, Springer International Publishing: Cham, Switzerland. DOI:10.1007/978-3-319-00690-1.
[47] J. F. Kiefner, "Fracture initiation," in Paper G, Proceedings of the 4th Symposium on Line Pipe Research, Pipeline Research Committee of the American Gas Association, Dallas, Texas, USA, AGA Catalogue, 1969, pp. G1–G36.
[48] R. W. E. Shannon, "The failure behaviour of line pipe defects," International Journal of Pressure Vessels and Piping, vol. 2, no. 4, pp. 243–255, 1974. https://doi.org/10.1016/0308-0161(74)90006-4.
[49] W. Kastner, E. Röhrich, W. Schmitt, and R. Steinbuch, "Critical crack sizes in ductile piping," International Journal of Pressure Vessels and Piping, vol. 9, no. 3, pp. 197–219, 1981. https://doi.org/10.1016/0308-0161(81)90002-8.
[50] J. Baek, Y. Kim, W. Kim, J. Koo, and C. Seok, "Load bearing capacity of API X65 pipe with dent defect under internal pressure and in-plane bending," Materials Science and Engineering: A, vol. 540, pp. 70–82, 2012, doi: 10.1016/j.msea.2012.01.078. https://doi.org/10.1016/j.msea.2012.01.078.
[51] C. T. Belachew, M. Che Ismail, and S. Karuppanan, "Strength assessment of corroded pipelines—Finite element simulations and parametric studies," International Journal of Structural Stability and Dynamics, vol. 17, no. 07, p. 1750069, 2017. DOI:10.1142/S0219455417500699.
[52] R. Amaya-Gómez, M. Sánchez-Silva, E. Bastidas-Arteaga, F. Schoefs, and F. Munoz, "Reliability assessments of corroded pipelines based on internal pressure–A review," Engineering Failure Analysis, vol. 98, pp. 190–214, 2019. https://doi.org/10.1016/j.engfailanal.2019.01.064.
[53] C. P. DNV, "Recommended Practice DNV-RP-F101," 2017, DNV Oslo, Norway.
[54] Y. H. Wang, G. Z. Wang, S. T. Tu, and F. Z. Xuan, "In-plane and out-of-plane constraint characterization of different constraint parameters for semi-elliptical surface cracks in pipes," Engineering Fracture Mechanics, vol. 235, p. 107161, 2020. https://doi.org/10.1016/j.engfracmech.2020.107161.
[55] K. M. Sujon, R. B. Hassan, Z. T. Towshi, M. A. Othman, M. A. Samad, and K. Choi, "When to Use Standardization and Normalization: Empirical Evidence from Machine Learning Models and XAI," IEEE Access, 2024. DOI: 10.1109/ACCESS.2024.3462434.
[56] J. Yu et al., "A confidence interval-based process optimization method using second-order polynomial regression analysis," Processes, vol. 8, no. 10, p. 1206, 2020. https://doi.org/10.3390/pr8101206.